INTERNATIONAL ATOMIC ENERGY AGENCY
UNITED NATIONS EDUCATIONAL, SCIENTIFIC AND CULTURAL ORGANIZATION
INTERNATIONAL CENTRE FOR THEORETICAL PHYSICS
I.C.T.P., P.O. BOX 586, 34100 TRIESTE, ITALY, CABLE: CENTRATOM TRIESTE

H4-SMR 393/66

SPRING COLLEGE ON PLASMA PHYSICS

15 May - 9 June 1989

COMPUTATIONAL PLASMA PHYSICS
Thermal Fluctuations & Noise in Plasma Simulation Models

R. D. Sydora

Department of Physics
University of California
Los Angeles
U. S. A.

ICTP Spring College on Plasma Physics
(May 15-June 19, 1989)

Lecture Notes in Computational Plasma Physics (by R.D. Sydora)

Lecture 1 : Thermal Fluctuations and Noise in Plasma Simulation Models.

Introduction to Plasma Simulation

It is a difficult task to review the progress and current areas of research in particle simulation of plasmas in such a short time. In order not to give a large volume of material and gloss over important and subtle details I chose to describe to you a couple of topics covered in some depth and I hope to impress upon you the amount of detailed structure and insight one can gain into plasmas with the tools of particle simulation. Before beginning, I would like to give the following references which are helpful for the self-learner and where some of the background of the topics I will present will be found. The references are:

(i) R. W. Hockney and J. Eastwood, "*Computer Simulation Using Particles*",McGraw-Hill, NY,(1981).
(ii) J.M. Dawson, "Particle Simulation of Plasmas", Rev. Mod. Phys.,55,403,(1983).
(iii) C.K. Birdsall and A.B. Langdon, "*Plasma Physics via Computer Simulation*",McGraw-Hill,NY,(1985).
(iv) T. Tajima, "*Computational Plasma Physics: With Applications to Fusion and Astrophysics*", Addison-Wesley, Redwood City, Ca., (1989).

The field of plasma simulation is rapidly evolving because of the progress in the development of supercomputers. In fact, plasma simulation always pushes to the limits of what is currently available. The simplest 1-D electrostatic model can easily fill the memory of the largest Cray or IBM computer with a few million particles and a few thousand grid points. These simple models can easily find the computing machine limits and its weak points. It is ever so important to be able to minimize the discreteness effects in plasma simulations by using many more particles and modes in order to approach a more collisionless limit, as described by the Vlasov equation.

Particle simulations began about thirty years ago, as you will note in the references, and they started out as a method used to examine collective plasma behavior in the kinetic regime, with virtually no approximations. What it has resulted in is a powerful tool for interpreting highly nonlinear kinetic effects like wave instabilities and associated plasma diffusion, heating and acceleration in such diverse areas as fusion research, space and astrophysics, industrial plasma processing (i.e. plasma etching and solid state plasmas) and more recently in advanced high energy plasma particle accelerators.

The plasma simulation models are now evolving in order to cover a wider range of spatial and temporal scales which reflects the hierarchical nature of the plasma. Since the rate at which computing speed and efficiency being made available to us is roughly known, it is still not possible for us to simulate many of the interesting regimes of the plasma and this has been the motivation for looking at long time scale simulation models. We must, however, carefully analyze the approximations which are made in order that the small (or large) scales we attempt to neglect do not affect the long time or large spatial scale we want to resolve. I would like to present some techniques for looking at the long time scale behavior of plasmas and consider a useful tool for investigating the particle dynamics on a 'microscopic' level. Before doing this a little background is needed and I summarize a few basics

Particle Simulation Model Basics

a) Finite-Size Particle Representation

This representation is physically motivated by the fact that with a Coulomb force law between a large number of interacting particles, the part of the force law which contains the slow fall-off with distance gives rise to collective behavior which we wish to simulate, and the short range part, which is huge and gives rise to collisional effects should be modified. In order to minimize the effects of two particles passing near each other and feeling this rapid variation the particles are treated as charge clouds with finite size, having no internal degrees of freedom. When the charge clouds are far apart the force is Coulombic but when they are near each other and begin to overlap this force goes to zero. The force on a particle centered at (x,v) is given by:

$$\underline{F}(\underline{x},\underline{v},t) = q\int d\underline{x}'\, S(\underline{x}'-\underline{x})\left[\underline{E}(\underline{x}',t) + \frac{1}{c}\underline{v}\times\underline{B}(\underline{x}',t)\right]$$

with corresponding charge and current densities given as:

$$\rho(\underline{x},t) = \int d\underline{x}'\, S(\underline{x}-\underline{x}')\,\rho_s(\underline{x}',t) \qquad \text{, normalize: } \int S(\underline{x})\,d^3\underline{x} = 1$$

$$\underline{J}(\underline{x},t) = \int d\underline{x}'\, S(\underline{x}-\underline{x}')\,\underline{J}_s(\underline{x}',t)$$

These equations are convolution integrals and lead to a natural interpretation in Fourier space:

$$\underline{F}(\underline{k},\underline{v},t) = q\, S(-\underline{k})\left[\underline{E}(\underline{k},t) + \frac{1}{c}\,\underline{v}\times\underline{B}(\underline{k},t)\right]$$

$$\rho(\underline{k},t) = S(\underline{k})\,\rho_s(\underline{k},t)$$

$$\underline{J}(\underline{k},t) = S(\underline{k})\,\underline{J}_s(\underline{k},t) \qquad , \quad S(\underline{k}) \equiv \int dx\, S(\underline{x})\, e^{-i\underline{k}\cdot\underline{x}}$$

(Gaussian particle $= e^{-a^2k^2/2}$)

The standard Vlasov and Fokker-Planck theory of plasmas can be and has been redone using this representation. In the sixties and seventies a great deal of effort was made to show this modifcation of the force law could lead to a plausible and physical representation of a collisionless or weakly collisional plasma. See the references for this development.

b) Components of Simulation Model

initialization

$$f_0(\underline{v}),\ n_0(\underline{x}) \longrightarrow (\underline{x},\underline{v})_i$$

- For $f(v)$, $P(v) = \int_{v_{min}}^{v} f(v)\,dv \,/\, \int_{v_{min}}^{v_{max}} f(v)\,dv$, and invert to get $V(P)$, and a random # P between 0 and 1 is taken to pick v_i
- For $n(x)$, $a \le x \le b$ given, form cumulative distribution:

$$N(x) = \int_a^x n(x')\,dx' \,/\, \int_a^b n(x')\,dx'$$

$N(x_i) = [0,1]$ (uniform distribution) $\qquad N(a) = 0,\ N(b) = 1$

Similarly for $f(\underline{v})$.

source accumulation (using dipole approx)

x_i = particle position, x_g = grid position

$$\rho(\underline{x}) = \sum_i S(\underline{x}-\underline{x}_i) \qquad , \quad x_i = x_g + (x_i - x_g)$$

(Taylor expand in $x_i - x_g$)

$$= \sum_i \left[S(\underline{x}-\underline{x}_g) + (\underline{x}_i-\underline{x}_g)\cdot\nabla_g S(\underline{x}-\underline{x}_g) + \frac{1}{2}(x_i-x_g)^2 : \nabla_g^2 S(\underline{x}-\underline{x}_g) + \cdots\right]$$

$$= \sum_g \sum_{i\in g}\left[S(\underline{x}-\underline{x}_g) + (\underline{x}_i-\underline{x}_g)\,S'(\underline{x}-\underline{x}_g) + \cdots\right]$$

field solution (k-space)

$$\rho(k_m) = \sum_{x_g} \rho(x_g)\, e^{-ik_m x_g} \qquad , \quad k_m = \frac{2\pi m}{L},\ m = 0, 1, \ldots, \pm\frac{L}{2}$$

Poisson eq. $\longrightarrow$ $E(k) = -i\frac{4\pi q}{k^2}\frac{\gamma(k)}{K^2}\rho(k)$ where $\begin{cases}\gamma(k) = \dfrac{\sin(kA)}{kA} \\ K^2 = \left(\dfrac{\sin(k\Delta/2)}{(k\Delta/2)}\right)^2\end{cases}$

accounts for use of spatial grid.

$E(x) = \text{FFT}^{-1}(E(k))$

force interpolation and particle mover

Force acting on i^{th} particle. $F(x_i) = q\int E(x+x_i)\,S(x)\,dx$

and in dipole approx., expanding x_i around x_g

$$F(x_i) = q\int\left[E(x+x_g) + (x_i - x_g)\cdot\nabla_g E(x+x_g)\right] S(x)\,dx$$

$$\frac{d\underline{v}_i}{dt} = \frac{\underline{F}_i}{m_i} + \frac{q}{m_i}\left(\frac{\underline{v}_i\times\underline{B}}{c}\right) \longrightarrow$$

$$\frac{d\underline{x}_i}{dt} = \underline{v}_i$$

Leapfrog scheme (a staggered mesh)

$$\frac{\underline{v}_i^{t_0+\Delta t/2} - \underline{v}_i^{t_0-\Delta t/2}}{\Delta t} = \frac{\underline{F}_i^{t_0}}{m} + \frac{q}{m}\left(\underline{v}_i^{t_0}\times\frac{\underline{B}^{t_0}}{c}\right)$$

$$\frac{\underline{x}_i^{t_0+\Delta t} - \underline{x}_i^{t_0}}{\Delta t} = \underline{v}_i^{t_0+\Delta t/2}$$

diagnostics

Time histories | particle | fields

$E_s = \frac{1}{8\pi}\int |E|^2 dx$ | $f(v,t)$ | $E(x,t)$

$T_K = \frac{1}{2}\sum_i m_i v_i^2$ | $T_{\perp,n}(x,t)$ | $\phi(x,t)$

$E_T = E_s + E_K$ | $J_{n,\perp}(x,t)$ | $\phi(k,\omega)$

$T_{n,\perp} = \left(\frac{v_{n,\perp}}{v_{n,\parallel}}\right)$ | $n_{e,i}(x,t)$ | $J\cdot E$

$T_{n,\perp,\parallel} = \sum_i^N v_{n,\perp,\parallel}^2 - \langle v_{n,\perp,\parallel}\rangle^2$

$D_{e,i} = \sum_i^N \frac{(\Delta x_i)^2}{\tau}$, $\Delta x_i = x - x_{gc}$

c) Classes of Models

This section gives an overview of some of the basics models used and how they have been extended to include a broader range of spatial and temporal scales.

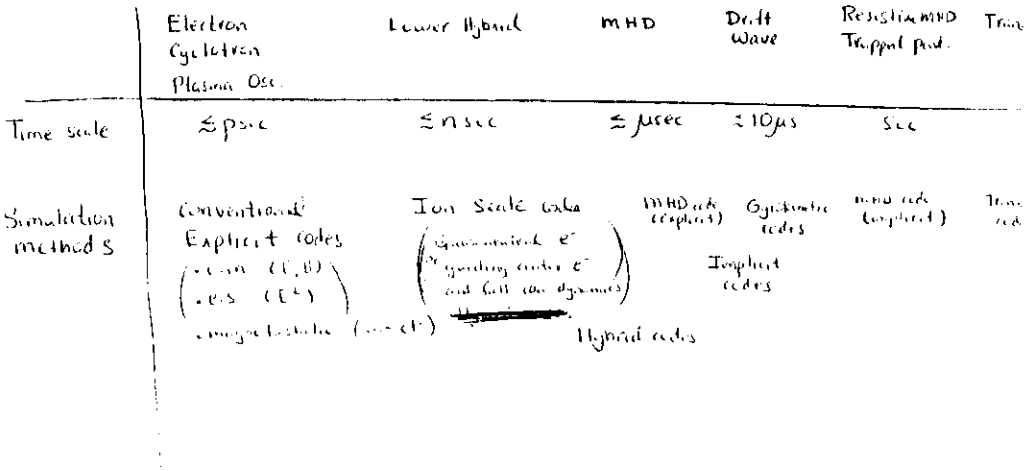

Noise Generation and Test Charges

The investigation of linear and nonlinear behavior in plasma simulation models can be very difficult due to the enhanced discreteness effects associated with the use of a finite number of particles. Diagnostics to demonstrate the correct physical behavior in simulation models are often made using two time correlation functions of the field quantities, such as the electrostatic potential and current, in order to determine the normal mode damping and frequency spectrum. Also, the time averaged field energy of each Fourier mode is measured in order to verify the correct equipartition of wave energy density.

More stringent tests on the simulation models such as the verification of the test particle behavior (i.e. dynamic shielding and friction) are more difficult due to the noise produced by the finite number of macro-particles as well as the errors in interpolation on a spatial grid which is used to mediate the particle interaction. Some effort has been given to the study of collisional processes in the finite-sized particle models [1,2], however, little effort has been given to quantifying the dynamic shielding and diffusion of individual test charges [3] which ultimately leads to the development of noise (incoherent spectral components) and collective effects in the simulations [4].

The particle simulations can be regarded more closely as a real experiment because the model is independent of any statistical assumptions. Statistical quantities such as the two point temporal and spatial correlations can be constructed from the data and compared with theories. Unlike real experiments, however, the numerical experiments are reproducible exactly but like a real experiment it can be difficult to extract the desired effects because of the large number of physical processes which occur. The concept of a test charge or test wave has

proved to be an important tool in the theoretical development of plasma kinetics. For instance in a thermal plasma one is interested in probing the response of the plasma to a test charge or current from an antenna or the effects of a test wave coupling to a turbulent bath of coupled waves and particles. These may be regarded as subtle effects generally difficult to measure with satisfactory statistical accuracy.

In this paper we present an alternative method for investigating subtle plasma behavior and this method is not based on a statistical formulation, but on the reproducibility of the simulation experiments. We use the physical process of dynamic shielding of test charges as an illustration of the technique and detail one can acheive in the dynamics of the model. In section 2 the diagnostic procedure is presented and we discuss the details of the implementation in simulation models. In section 3 examples are presented illustrating the utility of the method and how the technique is able to be used in verification of physical behavior in new models. In section 4 further applications are discussed and conclusions are given.

The Subtraction Method

The basic procedure in the subtraction technique is to perform two simulation runs with exactly the same initial conditions, however, in one of the runs a small perturbing influence is added such as an extra charge or small current. The resultant electric and magnetic field data from each run is retained at selected time steps and the two results are subtracted at each selected time step. In essence this may be regarded as the perfect data filter and if it is computationally feasible to perform many simulation runs with nearly the same initial conditions and subtract the results, then we are able to probe subtle processes which occur.

The procedure is not limited to small perturbations. Those effects in both simulations, which do not depend on the perturbation, will be identical in both runs and hence will be identically subtracted out. However, if the perturbation is strong, there will be little in the simulation which will depend on the perturbation and the subtraction is not necessary. This simple procedure can be extended in many ways. For instance, one could also perform a sequence of subtractions for a system with many different test charges or a system driven by a low amplitude source current at different wavenumbers and frequencies. The total perturbed plasma response would be given as:

$$\phi(\vec{r},t) = \phi_1(\vec{r},t) - \phi_j(\vec{r},t) \quad , \qquad j = 2, \ldots N \tag{1}$$

where ϕ_1 is the electrostatic potential, for example, of the reference run and the subscript j refers to runs with different perturbations. If one is interested in probing the response of the plasma at a certain scale, a test wave can be launched which may or may not be a normal mode of the system. The coupling of the test wave to other waves and its decay rate can be measured with good accuracy.

The subtraction method can be further generalized to the study of weakly unstable systems. A simulation run at thermal equilibrium can be made and a second run with the free energy source included can be subtracted.

Applications of the Method

Test Particle Shielding

A first application of the subtraction method has been to the problem of Debye screening of test particles. The test particle can be thought of as generating all ω and k's in the Fourier transform sense. The subtraction technique gives the plasma response and thus we can investigate the dielectric in detail. The

electrostatic potential surrounding a test charge moving at constant velocity, $\vec{v}$, is given by:

$$\phi(\omega,k) = \frac{-4\pi q_T e^{-i\vec{k}\cdot\vec{x}_o}}{ik^2(\omega - \vec{k}\cdot\vec{v})\epsilon(\omega,\vec{k})} \tag{2}$$

where the test charge density is $\rho(\vec{x},t) = q_T\delta(\vec{x} - \vec{x}_o - \vec{v}t)$ for $t > 0$. To obtain the response in $(\vec{x},t)$ space one first inverts the Laplace transform in time and applying Cauchy's theorem, integrates over $\vec{k}$, assuming poles at $\omega = \vec{k}\cdot\vec{v}$ and $\omega = \omega_j$, where ω_j are roots of the dielectric ϵ. This gives:

$$\phi(\vec{x},t) = \phi_D(\vec{x},t) + \phi_C(\vec{x},t) \tag{3}$$

with:

$$\phi_D(\vec{x},t) = 4\pi q_T \int_{-\infty}^{\infty} \frac{d^n k}{(2\pi)^n} \frac{e^{i\vec{k}\cdot(\vec{x}-\vec{x}_o-\vec{v}t)}}{k^2\epsilon(\vec{k},\vec{k}\cdot\vec{v})} \tag{3a}$$

$$\phi_C(\vec{x},t) = -4\pi q_T \sum_j \int_{-\infty}^{\infty} \frac{d^n k}{(2\pi)^n} \frac{e^{i\vec{k}\cdot(\vec{x}-\vec{x}_o)}e^{-i\omega_j t}}{k^2(\vec{k}\cdot\vec{v}-\omega_j)\frac{\partial\epsilon(\omega_j,\vec{k})}{\partial\omega}} \tag{3b}$$

where n is the spatial dimensionality [5]. The first term on the right hand side of equation (3) is the Debye cloud potential and the second term is the Cérenkov term which is usually neglected because ω_j is always damped. For modes near marginal stability ϕ_C can be larger than ϕ_D. If a cold plasma model is used for the dielectric response:

$$\epsilon(\omega,k) = 1 - \left(\frac{\omega_p}{\omega}\right)^2 \tag{4}$$

one obtains:

$$\phi_D(x,t) = \begin{cases} 0, & x > x_o + vt \\ \frac{4\pi q_T v}{\omega_p} sin\{\frac{\omega_p}{v}(x - x_o - vt)\}, & x < x_o + vt \end{cases} \tag{5}$$

$$\phi_C(x,t) = -2\pi q_T|x - x_o|cos(\omega_p t) \tag{6}$$
$$+ \begin{cases} \frac{-4\pi q_T v}{\omega_p} sin\{\frac{\omega_p}{v}(x - x_o - vt)\} - \frac{2\pi q_T v}{\omega_p} sin(\omega_p t), & x > x_o + vt \\ \frac{2\pi q_T v}{\omega_p} sin(\omega_p t), & x < x_o + vt \end{cases}$$

The unshielded potential, $2\pi q_T|x - x_o|$, which oscillates at $\omega = \omega_p$ is the plasma response to the sudden creation of a new charge at t=0. The oscillations at $\omega_p = kv$ is the excitation of the plasma wake by the test charge. The full kinetic solution of equation (3) for a test charge moving at $v = 3v_{te}$ is given in Figure 1. A large 'ringing' caused by the sudden creation of the test charge is evident and masks the wake behind the charge. This effect is prevalent even when the charge is turned on adiabatically and is also independent of the particle velocity. To rid this effect an electron-positron pair is created instead of a single test charge. One of the pairs moves to the right while the other is created at rest. This cancels the large 'ringing' and we are left with the plasma wave excited by the test charge as well as the polarization cloud around the stationary portion of the pair. These are shown in Figure 2 for four different velocity classes of particles. We next turn to the simulation results which are compared with the analytic predictions of test particle behavior.

A standard one-dimensional, electrostatic finite-sized particle-in-cell simulation model with second order spline functions for interpolating the charge and forces, was used to obtain the results. In the reference run the electrons were distributed uniformily in space with a Maxwellian velocity distribution from a Gaussian random number generator. The ions are assumed to be a fixed neutralizing background. In addition one extra test charge with zero velocity is included. A second run is prepared identically except that the extra test charge moves to the right with velocity v. The time evolution of the electrostatic potential at each point in space and time is recorded in each run and the difference between the two is displayed. Both periodic and vacuum boundary condtions have been used.

The agreement between theory and simulation is quite remarkable, especially at early times. Figure 3 illustrates the case of a test charge moving at $3v_{te}$ using the bounded model. At time step $\omega_p t = 40$ discreteness effects begin to occur and theoretical predictions show substantial deviation from the simulation. In this case $n\lambda_D = 4000$ and $\omega_p \Delta t = 0.2$. The discreteness effects observed in the simulation include the excitation of a precursor in front of the particle, an interference pattern in the wake indicating excitation of short wavelength modes in the wake and local growth or enhancement of the amplitude in parts of the wake.

A study of the properties of these effects has led to some understanding of their origin. The precursor does not depend on the test charge itself and the leading edge propagates near $4v_{te}$ which is the velocity of the fastest simulation particle. Therefore, the precursor is quite likely caused by background electrons traversing the wake behind the test charge, overtaking it, and because of the long time memory propagates the disturbance in front of the test charge. The enhancement of the short wavelength part of the spectrum behind the wake is thought to be due to collisions between two fast particles giving rise to electrostatic bremstralung [6]. Finally, the local growth in the plasma wake has been shown to depend only on the discreteness parameter, by making simulation runs with larger numbers of particles per cell, and therefore may depend on pre-existing fluctuation levels of the waves in the plasma.

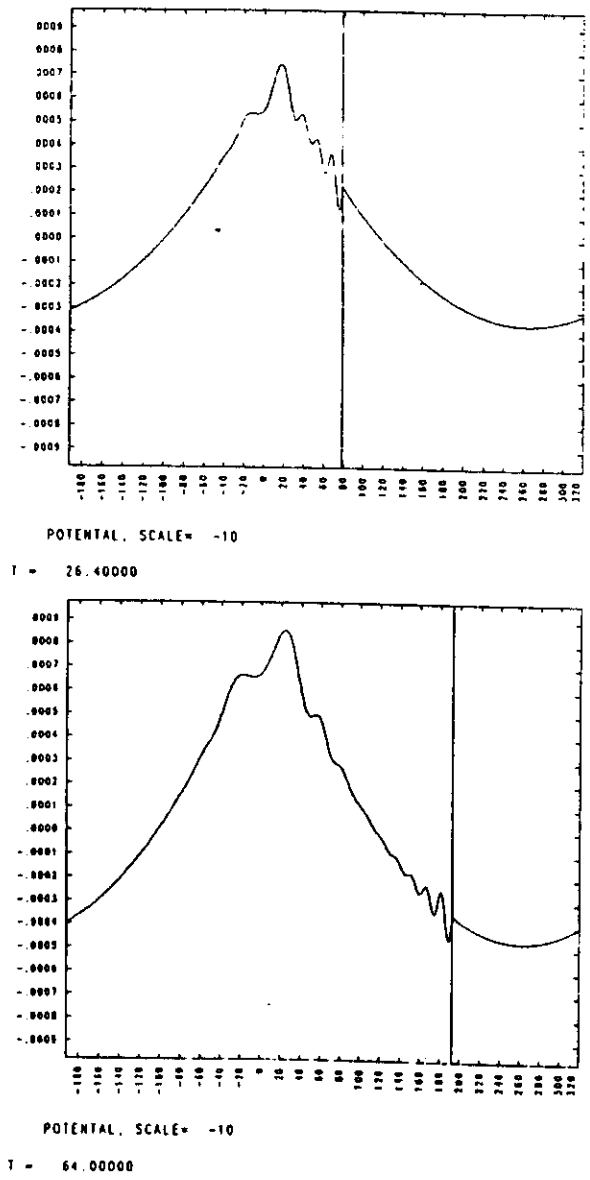

Fig. 1 Plasma wake emitted by one dimensional test charge moving at velocity $3v_{te}$ as predicted by kinetic theory. Vertical bar shows the location of the test charge and time is normalized to ω_{pe}^{-1}.

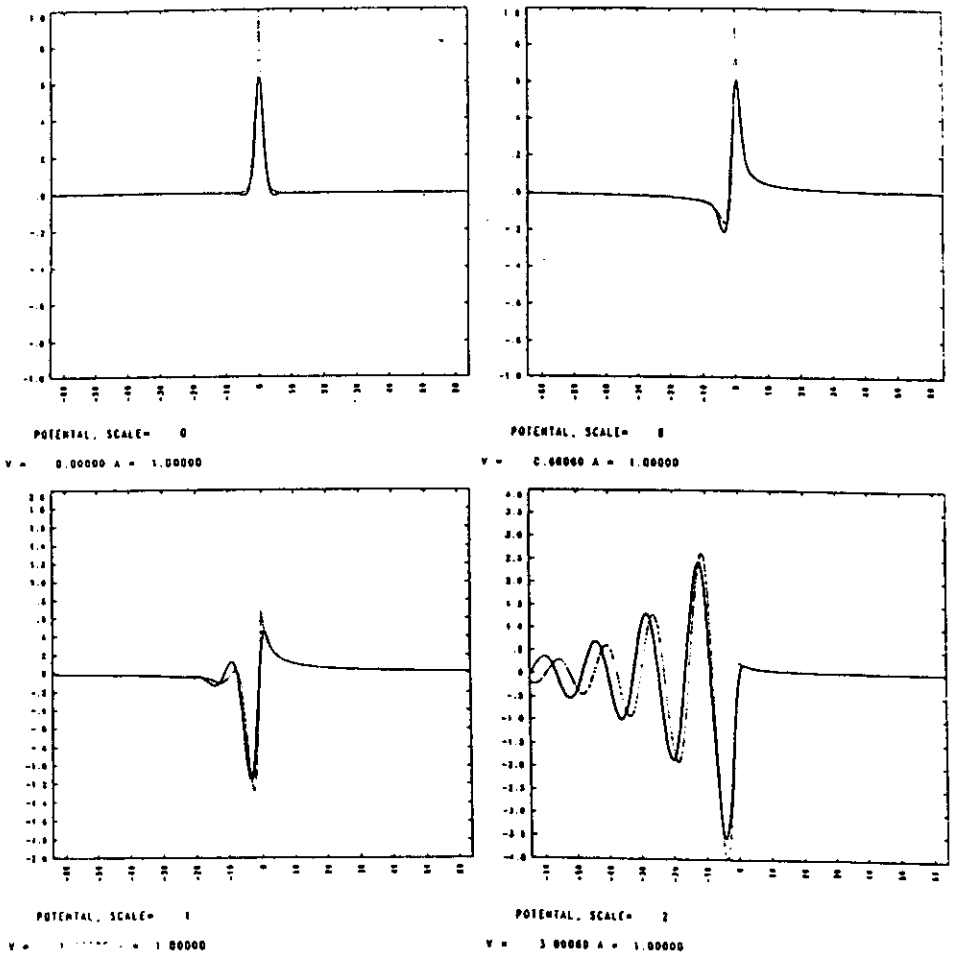

Fig. 2 Theoretical prediction of Debye shielding and wake behind a one dimensional test charge for various velocities. Solid line is the point particle result and dashed line is the finit-size particle result. The test charge is located at the center and moving to the right.

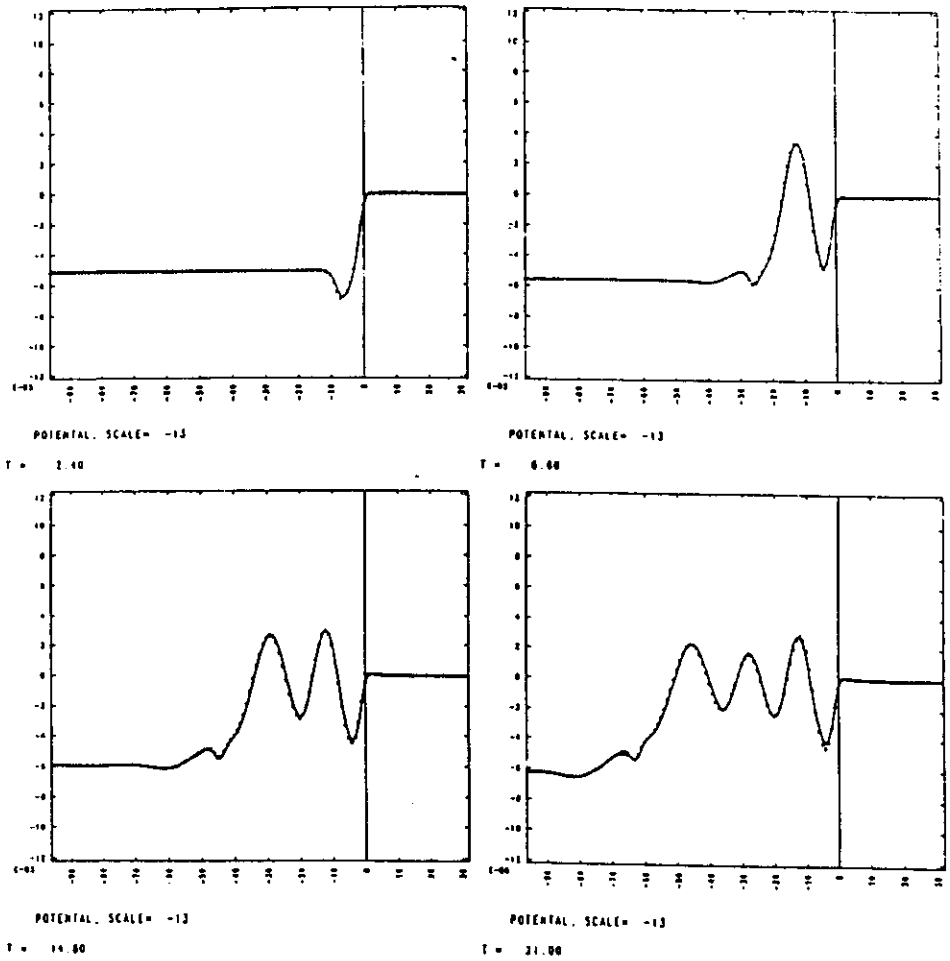

Fig. 3a Time evolution of the plasma wake behind test charge moving at velocity $3v_{th}$. Dots represent theory prediction and solid lines are the simulation result.

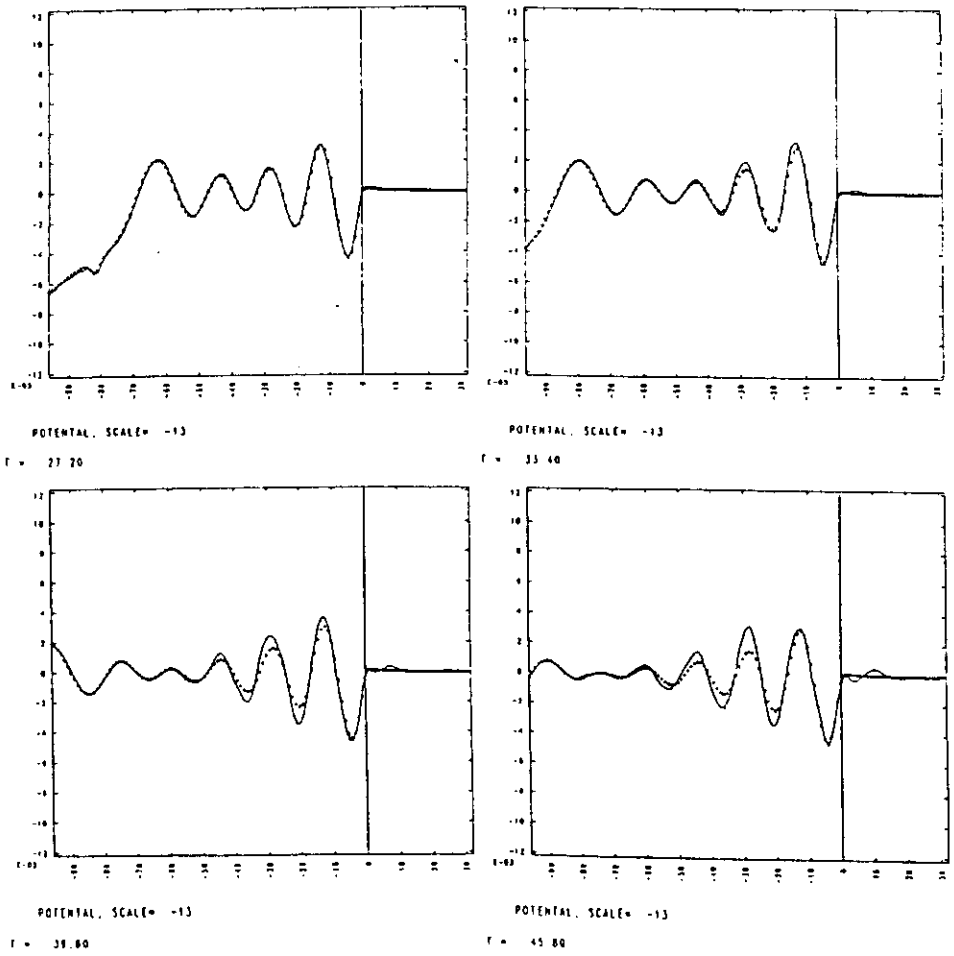
POTENTAL, SCALE= -13
T = 27.20
POTENTAL, SCALE= -13
T = 33.40
POTENTAL, SCALE= -13
T = 39.60
POTENTAL, SCALE= -13
T = 45.80

Fig. 3b

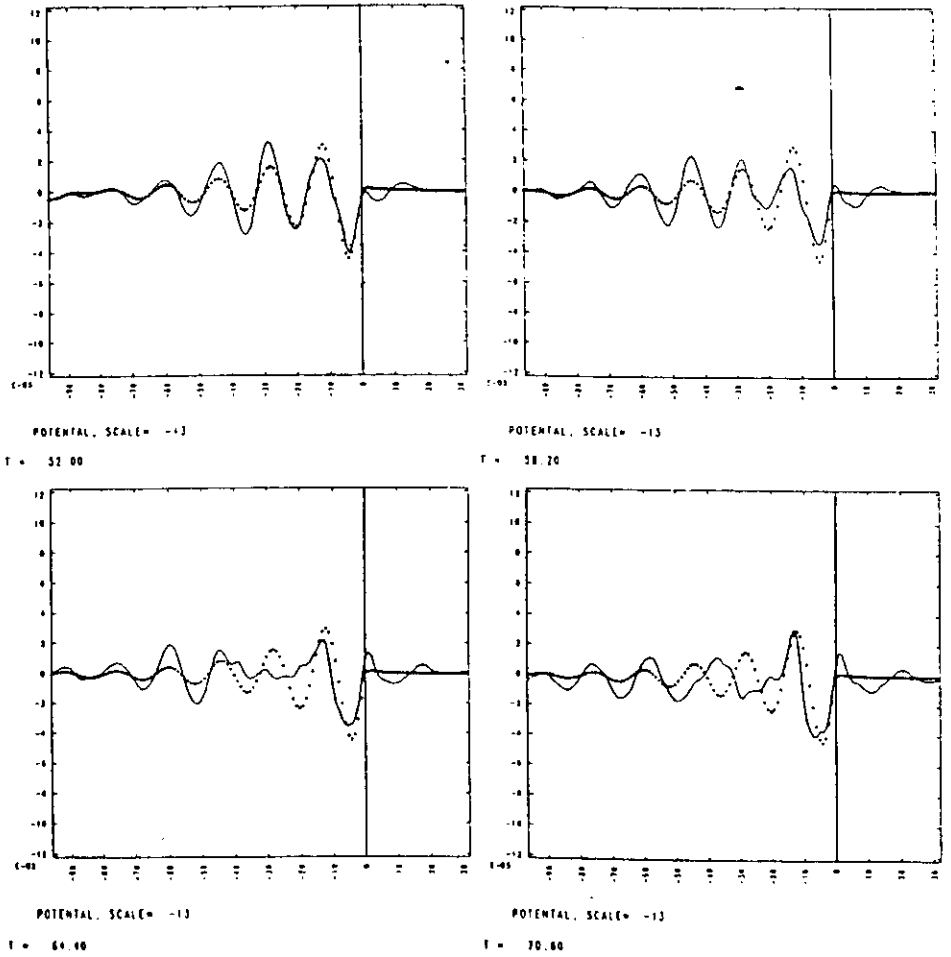
POTENTAL, SCALE= -13
T = 52.00
POTENTAL, SCALE= -13
T = 58.20
POTENTAL, SCALE= -13
T = 64.40
POTENTAL, SCALE= -13
T = 70.60

Fig. 3c

2D – magnetized Debye Clouds

Figure 12: simulation Debye cloud
$v = 0$

Figure 15: analytic Debye cloud
$v = 0$

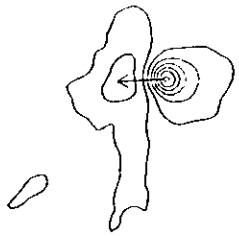

Figure 13: simulation Debye cloud
$v = 1.5$

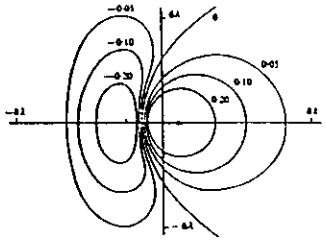

Figure 16: analytic Debye cloud
$v = 1.4$

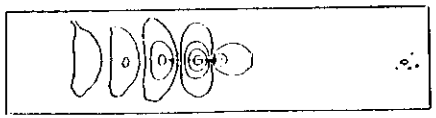

Figure 14: simulation Debye cloud
$v = 4$

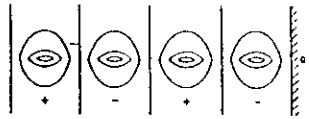

Figure 17: analytic Debye cloud
$v >> 1$

2D – magnetized Debye Clouds

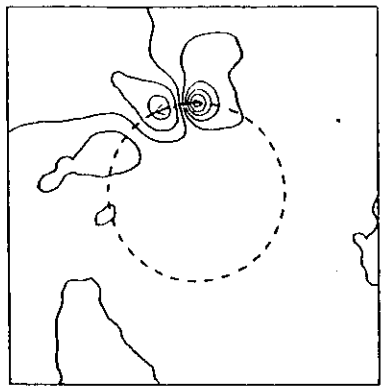

Figure 18: simulation Debye cloud
$V = 3v_T$, $\Omega = 0.4\omega_p$

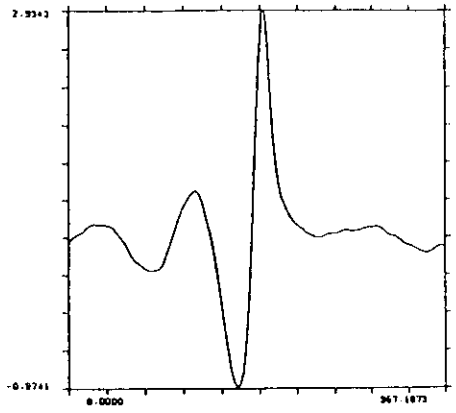

Figure 20: potential slice
$\rho = 7.5\lambda_D$

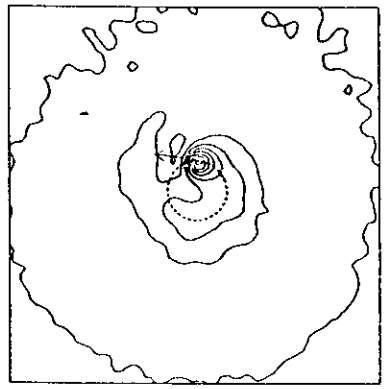

Figure 19: simulation Debye cloud
$V = 1v_T$, $\Omega = 0.4\omega_p$

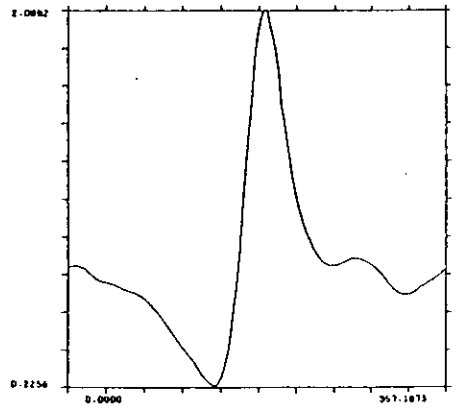

Figure 21: potential slice
$\rho = 2.5\lambda_D$

References

[1] Okuda, H., and Birdsall, C.K., *Phys. Fluids* **13**, 2123-2134,(1970).

[2] Okuda, H., *Phys. Fluids* **15**, 1268-1274.(1972).

[3] Langdon, A.B., and Birdsall, C.K., *Phys. Fluids* **13**, 2115-2122,(1970).

[4] Langdon, A.B., *Phys. Fluids* **22**, 163-171.(1979).

[5] Krall, N.A., and Trivelpiece, A.W., *Principles of Plasma Physics*, McGraw-Hill, NY, (1973).

[6] Dawson, J.M., Shanny, R., and Birmingham, T.J., *Phys. Fluids* 12.687-693,(1969).

[7] Birdsall, C. K. and Langdon, A. B., *Plasma Physics via Computer Simulation*, McGraw-Hill, NY, (1985).

[8] Friedman, A., Langdon, A.B., and Cohen, B.I., *Comments Plasma Phys. Control. Fusion* 6.225-236.(1981).

[9] Barnes, D.C., Kamimura, T., Leboeuf, J. N., and Tajima, T., *J. Comp. Phys.* **52**, 480-502, (1983).

[10] Lee, W.W., *Phys. Fluids* **26**, 556-570.(1983).

Lecture 2 : Large Time Step Plasma Simulation Models with Applications

Introduction

Due to the enormous range of spatial and temporal scales in a plasma realistic simulations are difficult. Therefore, one approach is to use multiple time scale methods. The differential equations we must use become 'stiff' since the phenomena of interest develope on slow time scales even though the system supports high frequency normal modes.

The easiest way to master the basics of applying these methods is to look at the harmonic oscillator and its normal modes in order to get a feel for how to filter out high frequencies. Then add the plasma to filter out short wavelengths.

Useful references to begin with include:

(i) A B. Langdon, J. Comp. Phys., **30**, 202,(1979).

(ii) J. Denavit, J. Comp. Phys., **42**, 337,(1981).

(iii) A. Friedman et. al., Comm. on Plasma Physics and Controlled Fus., 6,225,(1981).

In this lecture I will follow the development of implicit methods in particle simulations and discuss the modifications to the test particle picture of the simulation plasma.

(I) Introduction and References

- enormous range of space and time scales in plasmas ⇒ makes realistic simulations difficult
- two examples to give feeling for this difficulty

(i) Laser Fusion

phenomena	light propagation + scattering (collisionless)	collisional electron kinetics	hydrodynamic effects
time scale	$\sim 10^{-15} - 10^{-13}$ sec	$\sim 10^{-13} - 10^{-10}$ sec ($\sim \tau_{ei}$)	$10^{-10} - 10^{-8}$ sec ($\sim R/c_s$)
length scale	$\sim 10^{-2} - 3\,\mu m$	$\sim 3 - 40\,\mu m$	$40 - 300\,\mu m$
Simulation method	conventional time centered meth.	Hybrid and moment meth.	particle-fluid and hydro. codes

(ii) Magnetic Confinement

phenomena	Electron cyclotron + plasma wave microinst. (ECRH)	Ion cyclotron + ion microinst. (ICRF)	Drift wave ion bounce (anomalous transport)	MHD (Resistive	Transp
time scale	$\sim 10^{-12} - 10^{-8}$ sec (ω_{ce}^{-1})	$\sim 10^{-8} - 10^{-6}$ sec (ω_{ci}^{-1})	$\sim 10^{-7} - 10^{-3}$ sec ω_b^{-1}	$\sim 10^{-4}$ - 1 msec τ_{ei}	$\sim 10^{-3}$ - 1 τ_{ii}
length scale	$\sim 10^{-3} - 10^{-2}$ cm (ρ_e)	$\sim 1 - 5$ cm (ρ_i)	$\sim 1 - 10$ cm $k\rho_i \sim 1$	10cm - 1 $k\rho_i < 1$	1
Simulation method	Conventional time centered method	Full ion dynamics + massless e^- (Fokker Planck)	Guiding center + gyroaveraged methods (Drift-Kinetic)	Full MHD Eq.	Transp code

- must employ multiple-time-scale methods
- differential equations become 'stiff', i.e. phenomena of interest develope on slow time scales even though system supports high frequency normal modes.
- to understand implicit methods must first understand harmonic oscillator and its normal modes.
- historical development / relevant papers to read

Ref:

*① A.B. Langdon, J.C.P., 30, 202 (1979)

② J. Denavit, J.C.P., 42, 337 (1981)

③ R.J. mason, J.C.P., 41, 233 (1981)

*④ A. Friedman, et.al., Comm. on Plasma Physics and Controlled Fusion, 6, 225 (1981)

⑤ D.C. Barnes et.al., J.C.P., 52, 480 (1983)

⑥ J. Brackbill and D. Forslund, J.C.P., 46, 271 (1982)

⑦ A.B. Langdon and D. Barnes, Comp. Physics Techniques, 'multiple Time Scale methods', 1985

(II) Harmonic Oscillator

- general case $F \propto X$

$$\begin{cases} V^{n+1} = V^n - \omega_p^2 \Delta t \, X^{n+\alpha} \\ X^{n+3/2} = X^{n+1/2} + \Delta t \, V^{n+1/2+\alpha} \end{cases}$$

- propagator $Z \sim e^{i\omega\Delta t} \Rightarrow$ amplification $\begin{pmatrix} V^n \\ X^{n+1/2} \end{pmatrix} = Z^n \begin{pmatrix} V \\ X \end{pmatrix}$

$$Z^{n+1} V = Z^n V - \omega_p^2 \Delta t \, Z^{n+\alpha-1/2} X$$

$$Z^{n+1} X = Z^n X + \Delta t \, Z^{n+\alpha+1/2} V$$

- dispersion relation

$$\begin{vmatrix} Z-1 & \omega_p^2 \Delta t \, Z^{\alpha-1/2} \\ -\Delta t Z^{\alpha+1/2} & Z-1 \end{vmatrix} = (Z-1)^2 + \omega_p^2 \Delta t^2 Z^{2\alpha} = 0$$

$$\boxed{(Z-1)^2 + (Z^{2\alpha}-1)\omega_p^2 \Delta t^2 + \omega_p^2 \Delta t^2 = 0} \quad (*)$$

- consider special cases:

a) Leapfrog ($\alpha = 1/2$)

$$(Z-1)^2 + (Z-1)\omega_p^2 \Delta t^2 + \omega_p^2 \Delta t^2 = 0$$

$$Z \sim e^{\pm i\omega_p \Delta t} + O(\omega_p^3 \Delta t^3)$$

$|Z| = 1$

$\omega_p \Delta t < 2 \Rightarrow$ stable (i.e. on circle)

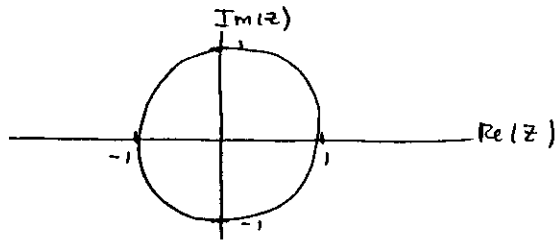

b) Fully Implicit ($\alpha = 1$)

$$(Z-1)^2 + (Z^2-1)\omega_p^2 \Delta t^2 + \omega_p^2 \Delta t^2 = 0$$

$$Z^2(1+\omega_p^2 \Delta t^2) - 2Z + 1 = 0$$

$$Z = \frac{1}{1+\omega_p^2 \Delta t^2} \pm \frac{i\omega_p \Delta t}{1+\omega_p^2 \Delta t^2}$$

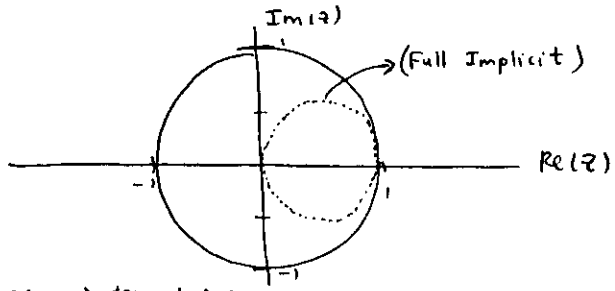

$\omega_p \Delta t$ arbitrary $\Rightarrow$ damped but stable

- would like to make bridge between full implicit and leapfrog

$$V^{n+1} = V^n - \omega_p^2 \Delta t \, \bar{X}^{n+1/2} \qquad \text{(decenter)}$$

$$X^{n+3/2} = X^{n+1/2} + \Delta t \, V^{n+1} \qquad \text{(center)}$$

where $\bar{X}^{n+1/2} = f(X^{n+3/2})$

- amplification

$$(z-1)V + \omega_p^2 \Delta t \, f(z) X = 0$$

$$-\Delta t z V + (z-1) X = 0$$

$$\boxed{(z-1)^2 + \omega_p^2 \Delta t^2 f(z) z = 0}$$

$f(z)$: Time filter or transfer function

optimum filter: $\bar{X}^{n+1/2} = \begin{cases} X^{n+1/2}, & \omega_{max} > \omega_p \\ 0, & \omega_{max} < \omega_p \end{cases}$

Note:

$f(z) = z \longleftrightarrow$ full implicit ($\alpha = 1$) or $\bar{X}^{n+1/2} = X^{n+1}$

(First order accurate)

- better filters (2nd order accurate)

Transfer functions:

$$f(z) = z^2/(2z-1) \longleftrightarrow \bar{X}^{n+1/2} = \frac{1}{2}(X^{n+3/2} + \bar{X}^{n-1/2})$$

$$f(z) = z^3 - (z-1)^3 - \frac{(z-1)^2}{2} \longleftrightarrow \bar{X}^{n+1/2} = \frac{2}{5}(X^{n+3/2} + 2\bar{X}^{n-1/2} - \frac{1}{2}\bar{X}^{n-3/2})$$

$$f(z) = \frac{z^2}{2z-1} \Longrightarrow z^3(2 + \omega_p^2 \Delta t^2) - 5z^2 + 4z - 1 = 0$$

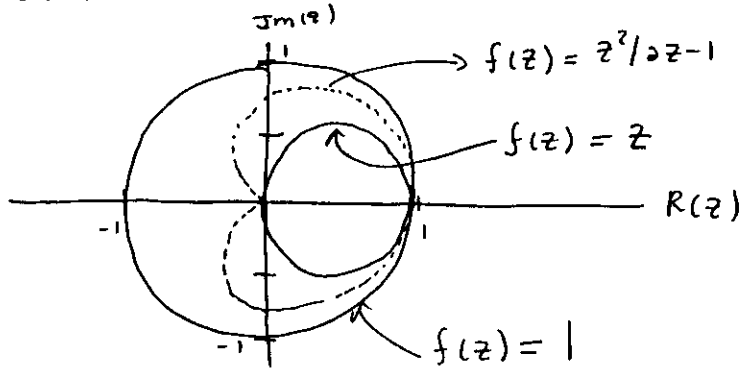

c) Explicit – Backward Biased ($\alpha = 0$)

From Eq. ⊛

$$(z-1)^2 + \omega_p^2 \Delta t^2 = 0$$

$$z = 1 + i\omega_p \Delta t \qquad \text{(Always unstable)}$$

$|z| > 1$

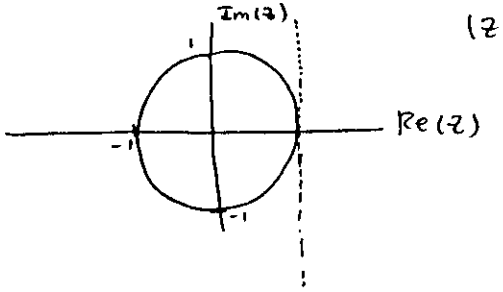

$$\begin{cases} V^{n+1} = V^n - \omega_p^2 \Delta t\, X^n \\ X^{n+3/2} = X^{n+1/2} + \Delta t\, V^{n+1/2} \end{cases}$$

Both decentered and depend on past values

$$\begin{cases} V^{n+1} = V^n - \omega_p^2 \Delta t\, X^n \\ X^{n+1} = X^n + \Delta t\, V^n \end{cases}$$

- Try to improve to 2nd order accuracy

Step ahead

$$X^{n+2} = X^n + \Delta t\, V^n + \Delta t V^n - \omega_p^2 \Delta t^2 X^n$$

$$V^{n+2} = V^n - \omega_p^2 \Delta t\, X^n - \omega_p^2 \Delta t\, X^n - \omega_p^2 \Delta t^2 V^n$$

- Take 1 step of $2\Delta t$

$$\tilde{X}^{n+2} = X^n + 2\Delta t\, V^n$$

$$\tilde{V}^{n+2} = V^n - 2\Delta t\, \omega_p^2 X^n$$

- Subtracting

$$\tilde{X}^{n+2} - X^{n+2} = \omega_p^2 \Delta t^2 X^n \qquad \therefore \text{error} \propto \omega_p^2 \Delta t^2$$

$$\tilde{V}^{n+2} - V^{n+2} = \omega_p^2 \Delta t^2 V^n$$

- correction to eliminate error

$$X^{n+1} = X^n + V^n \Delta t - \frac{\omega_p^2 \Delta t^2}{2} X^n$$

$$V^{n+1} = V^n - \omega_p^2 \Delta t\, X^n - V^n \frac{\omega_p^2 \Delta t^2}{2}$$

- amplification

$$z = 1 - \frac{\omega_p^2 \Delta t^2}{2} \pm i\omega_p \Delta t$$

$$|z|^2 = zz^*$$

$$= \left(1 - \frac{\omega_p^2 \Delta t^2}{2}\right)^2 + \omega_p^2 \Delta t^2$$

$$= 1 + \omega_p^4 \Delta t^4 / 4$$

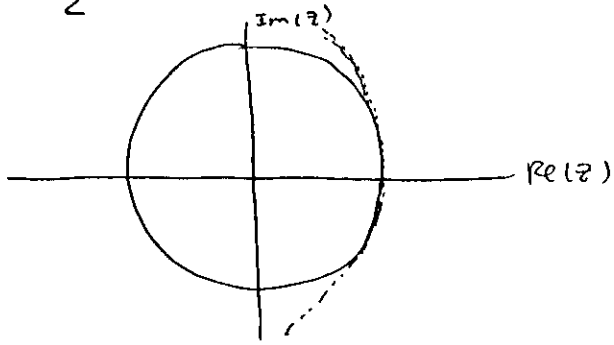

(Less unstable)

(III) Unmagnetized Plasma

a) Direct method

(i) Leapfrog ($\alpha = 1/2$) — (Acc. to $\omega_p^2 \Delta t^2$) 2nd order

$$\begin{cases} V_j^{n+1} = V_j^n + \dfrac{\Delta t\, q_j}{m_j} F_j^{n+1/2} \\ X_j^{n+3/2} = X_j^{n+1/2} + \Delta t\, V_j^{n+1} \end{cases}$$

$$F_j^{n+1/2} = \int S(x' - x_j^{n+1/2})\, E^{n+1/2}(x')\, dx'$$

Poisson Eq.

$$\nabla \cdot E^{n+1/2} = 4\pi \sum_j q_j\, S(x - x_j^{n+1/2})$$

(ii) Full implicit ($\alpha = 1$) — (Acc. to $\omega_p \Delta t$) 1st order

$$V_j^{n+1} = V_j^n + \frac{\Delta t\, q_j}{m_j} F_j^{n+1}$$

$$X_j^{n+3/2} = X_j^{n+1/2} + \Delta t\, V_j^{n+1}$$

$$F_j^{n+1} = \int S(x' - x_j^{n+1/2})\, E^{n+3/2}(x')\, dx'$$

Poisson Eq.

$$\nabla \cdot E^{n+3/2} = 4\pi \sum_j q_j\, S(x - x_j^{n+3/2})$$

- modified Poisson Eq.

$$\nabla \cdot E^{n+3/2} = 4\pi \sum_j q_j\, S(x - x_j^{n+3/2})$$

$$= 4\pi \sum_j q_j\, S(x - x_j^{n+1/2} - \Delta t\, V_j^{n+1})$$

$$= 4\pi \sum_j q_j\, S(x - x_j^{n+1/2} - \Delta t\, V_j^n - \Delta t^2 \frac{q_j}{m_j} \int dx' S(x' - x_j^{n+1/2}) E^{n+3/2}(x')\, dx'$$

$$\approx 4\pi \sum_j q_j\, S(x - x_j^{n+1/2} - \Delta t\, V_j^n) - 4\pi \sum_j q_j^2 \frac{\Delta t^2}{m_j} \frac{\partial}{\partial x} \int S(x' - x_j^{n+1/2}) E^{n+3/2}(x')\, dx'$$

- Nonlinear Eq.

$$\nabla \cdot E^{n+3/2} + 4\pi \sum_j q_j^2 \frac{\Delta t^2}{m_j} \frac{\partial}{\partial x} \int S(x' - x_j^{n+1/2}) E^{n+3/2}(x')\, dx'$$

$$\simeq 4\pi \sum_j q_j\, S(x - x_j^{n+1/2} - \Delta t\, V_j^n)$$

(Solve iteratively)

push particles

$$V_j^{n+1} = V_j^n + \frac{\Delta t\, q_j}{m_j} \int S(x' - x_j^{n+1/2}) E^{n+3/2}(x')\, dx'$$

$$X_j^{n+3/2} = X_j^{n+1/2} + \Delta t\, V_j^{n+1}$$

(iii) Implicit (2nd order accurate)

$$\begin{cases} V^{n+1} = V^n + \Delta t \frac{q_j}{m_j} \int dx' \, S(x' - x_j^{n+1/2}) \, \bar{E}^{n+1/2}(x') \\ X^{n+3/2} = X^{n+1/2} + \Delta t \, V^{n+1} \end{cases}$$

$$\bar{E}^{n+1/2} = \frac{1}{2}\left(E^{n+3/2} + \bar{E}^{n-1/2}\right)$$

Moment Implicit method

(i) 1st order accurate Implicit ($\alpha = 0$)

- just multiply above eqs. by v and f constructing moments

$$J_\alpha^{n+1} = J_\alpha^n - \frac{\Delta t}{m_\alpha}\left(\nabla_x \Pi_\alpha^n - q_\alpha n_\alpha E^{n+1}\right)$$

$$\Pi_\alpha = P_\alpha + n_\alpha m_\alpha u_\alpha^2 \quad (= n_\alpha k T_\alpha)$$

$$n_\alpha^{n+3/2} = n_\alpha^{n+1/2} - \Delta t \nabla_x J_\alpha^{n+1}$$

$$\nabla \cdot \bar{E}^{n+1} = 4\pi \sum_\alpha q_\alpha n_\alpha^{n+1}$$

c) Fluctuation - Dissipation Properties

- problems / drawbacks which must be understood before applying

(i) Aliasing instability

Leapfrog $\Rightarrow$ $\omega_{pe}\Delta t < 2$, $k V_{Th} \Delta t < 1$

Direct Implicit $\Rightarrow$ $\omega_{pe}\Delta t$ arbitrary , $k V_{Th} \Delta t \lesssim 1$

Moment Implicit $\Rightarrow$ $\omega_{pe}\Delta t$ arbitrary , $k V_{Th} \Delta t < 1$

(ii) Energy conservation and cooling

2 nonphysical processes:
- Nonresonant contributions to polarization drag
- nonresonant contributions to dynamical friction

cooling rate $\propto$ 1/ Number of modes

- Fokker Planck Eq. in Lenard Balescu form

$$\frac{\partial f}{\partial t} = \frac{\partial}{\partial v}\left(-f \langle a\rangle_{pol}\right) + \frac{\partial}{\partial v}\left(f \langle a\rangle_{diff}\right) + \frac{\partial}{\partial v}\left(\frac{\partial}{\partial v} f D\right)$$

$$\langle a\rangle_{\substack{pol \\ (drag)}} = \frac{q^2}{m}\int \frac{dk}{(2\pi)^3}\frac{\underline{k}}{k^2}\ \mathrm{Im}\left(\frac{1}{\epsilon(\underline{k}, \underline{k}\cdot\underline{v})}\right)$$

$$\epsilon = 1 + \omega_p^2 \int dv\ f_0(v)\left[\ \frac{X}{A}\ \right]$$

$$\mathrm{Im}(X/A) \sim -\pi\,\delta'(\omega - kv) + \text{non-res.}\ (\sim \cos\omega + \sin\omega$$

$$\langle a\rangle_{\substack{dynamic \\ friction}} = \frac{q^2}{m^2}\int \frac{dk}{(2\pi)^3}\frac{d\omega}{2\pi}\ \underline{k}\cdot(\underline{E}\underline{E})_{k,\omega}\ \mathrm{Im}\left(\frac{X}{A}\right)$$

[redacted]

(IV) Applications

- moment implicit — hot e^- emission in laser-foil targets
  - laser-induced transport
- direct method — ion acoustic instabilities
  - ion beam instabilities.

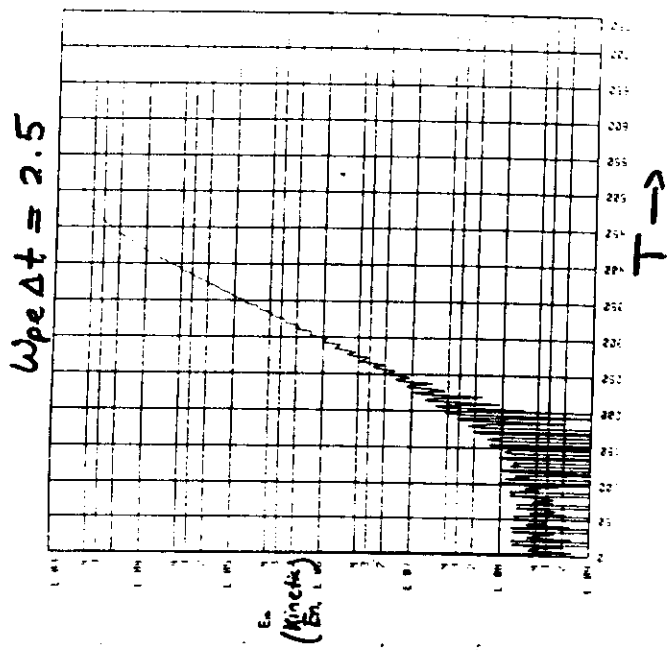

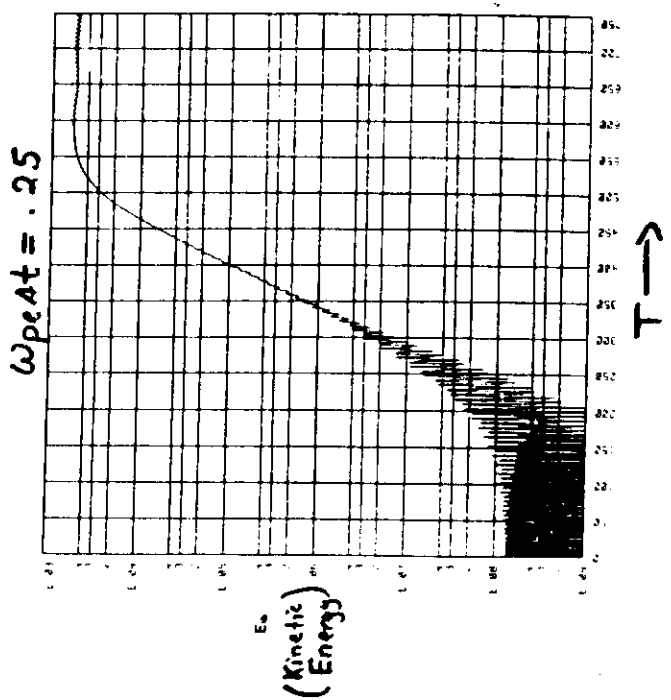

$n_0 = 256$ particles.

We now turn to an application of the subtraction method to long time step plasma simulation models. In particular, the direct implicit particle model, and for simplicity one dimensional models are considered, however generalizations of the procedures to two and three dimensions is straightforward [7].

In the direct implicit algorithm the particle mover is decentered in such a way as to lengthen the time step and this results in equations of motion resembling a slightly damped harmonic oscillator. In order to produce normal mode damping at certain scales while leaving others undamped, a modified Poisson equation is constructed. The implicit particle codes are not energy conserving because damped equations of motion are used, although acceptable values of energy conservation can be acheived. The physical sources of nonconservation are important to understand and in this section the subtraction method is used as a more intuitive approach since unphysical modifications are introduced by the finite time step that depend on wavelength and particle velocity. The Balescu-Lenard equation can be written for the plasma medium which supports lower frequency oscillations and damps out the high frequency components but the physicai processes are buried in the mathematical details and it not easy to determine which physical process dominates.

When finite time step and spatial grid effects are included in the kinetic description of simulation plasmas, white noise effects appear at the shortest wavelengths since thermal particles move a large fraction of a wavelength in one time step. At very large time steps the spectral behavior begins to upset the balance between velocity diffusion and drag which preserves energy in thermal equilibrium. This imbalance is mainly due to nonresonant polarization drag and dynamical friction effects which arise from phase errors in the damping [7].

Although comparison tests between full dynamic and direct implicit models have been made by Friedman et. al. [8] for the case of two stream instability, the thermal properties of the simulation model have not been adequately under-

stood. For our investigation we use first and second order direct implicit schemes which are not exactly momentum conserving since filtering is done on the mesh electrostatic potential rather than on the particle quantity [9]. It is more difficult to quantify the damping due to phase errors in such algorithms from an analytical approach and therefore the subtraction method aids us in this as well as understanding the physical origins of the damping. The form of the equations of motion is given by:

$$x_i^{n+3/2} = x_i^{n-1/2} + \Delta t v_i^{n-1} \tag{7a}$$

$$v_i^{n+1} = v_i^n + \Delta t \frac{q_i}{m_i} \int S(x' - x_i^{n-1/2}) E^{n+3/2}(x') dx' \tag{7b}$$

where S is the particle shape factor. The Poisson equation becomes:

$$\frac{\partial E^{n-3/2}(x)}{\partial x} + \sum_j 4\pi \frac{q_j^2}{m_j} \Delta t^2 \frac{\partial}{\partial x} S(x - x_j^1) \int dx' S(x' - x_j^{n-1/2}) E^{n-3/2}(x') \tag{7c}$$

$$= 4\pi \sum_j q_j S(x - x_j^1)$$

where we have expanded $S(x^{n+3/2})$ in a Taylor series about the free streaming position $x_j^1 = x_j^{n+1/2} + v_j^n \Delta t$. This nonlinear Poissson equation is solved iteratively in k-space and the convolutions are performed in real space. This scheme corresponds to the full implicit scheme and converges provided $\frac{\Delta x}{\Delta t^2} > (dv_i/dt)_{max}$ is satisfied.

A modification of the above scheme can make the algorithm second order accurate [9]. This is done by replacing equation (7b) with:

$$v_i^{n+1} = v_i^n + \Delta t \frac{q_i}{m_i} \int dx' S(x' - x_i^{n+1/2}) (E^{n-1/2}(x')) \tag{8}$$

where $(\,)$ denotes a time average and is given as:

$$(E^{n+1/2}) = \frac{1}{2}(E^{n-3/2} + (E^{n-1/2})) \tag{9}$$

The Poisson equation becomes:

$$\frac{\partial E^{n+3/2}(x)}{\partial x} + 2\pi \frac{\partial}{\partial x} \sum_j \frac{\Delta t^2 q_j^2}{m_j} S(x - x_j^{n+1/2}) \int dx' S(x' - x_j^{n+1/2}) (E^{n+3/2}(x') + (E^{n-1/2}(x')))$$

$$= 4\pi \sum_j q_j S(x - x_j^{n+1/2}) - 4\pi \Delta t \frac{\partial}{\partial x} \sum_j q_j v_j^n S(x - x_j^n) + 4\pi \Delta t \frac{\partial^2}{\partial x^2} \sum_j q_j (v_j^{n-1/2})^2 S(x - x_j^{n+1/2}) \tag{10}$$

The results of the simulations were made using system size, $L = 512\Delta = n\lambda_D = 100$, $v_{te} = 0.1 - 1$, and particle size, $a = 1.5\Delta - 2.2\Delta$. The time step was varied between $\omega_p \Delta t = 0.2 - 10$. Quadratic spline interpolation was used for the interpolation of the forces and charge density. The test charges were introduced the same way as described in the previous section and test particle velocities $v_{test} = 0.25$,1, and $3v_{te}$ were considered.

Figure 4 shows the results of the electrostatic potential from the subtraction method for a particle moving at $3v_{te}$ and with three different time step values. The results of the implicit code simulations were identical to the previous time-centered results with $\omega_p \Delta t = 0.2$. As an illustration of the detailed behavior one can explore with the subtraction method, Figure 4a is a comparison of test particle wakes using the subtracted dipole scheme and the more accurate quadratic spline interpolation. It is evident that the interpolation scheme accuracy as well as noise contributions can be quantified in a detailed manner. The overall shielding behavior is similar to the results of the previous section but in the larger time step runs ,as shown in Figure 4b, the short wavelengths in the wake are not prevalent. There are modulations in the wake amplitude as before, however, the electrostatic bremstralung contributions are weaker for larger time steps.

The results of nonphysical behavior for the largest time step, $\omega_p \Delta t = 10$, is shown in Figure 4b. It is evident from the comparison with the $\omega_p \Delta t = 2$ case

that there is over-enhanced shielding and the size of the Debye cloud increases with increasing time step. There is a strong cooling of the plasma and energy is no longer conserved. The dominant cooling arises from wave emission by the fast particles which in turn suffer the largest numerical damping. Measurement of the slope of the potential at the particle location gives an approximate measure of the self-forces on the particle and it is found that this increases approximately linearly with increasing time step. Further studies to evaluate the self-fields of the particles and comparsion with instantaneous wave emission studies for the implicit models are currently being pursued.

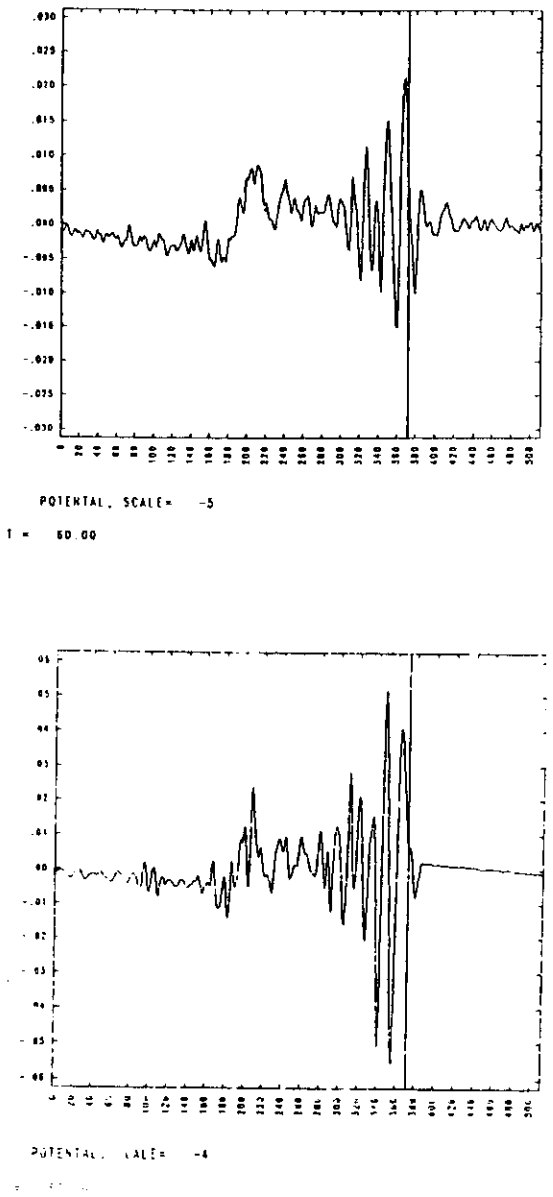

Fig. 4a Plasma wake emitted by one dimensional test charge moving at velocity $3v_{th}$ using direct implicit model. Time step used is $\omega_p \Delta t = 0.2$. Top panel is result using subtracted dipole scheme and bottom is quadratic spline interpolation.

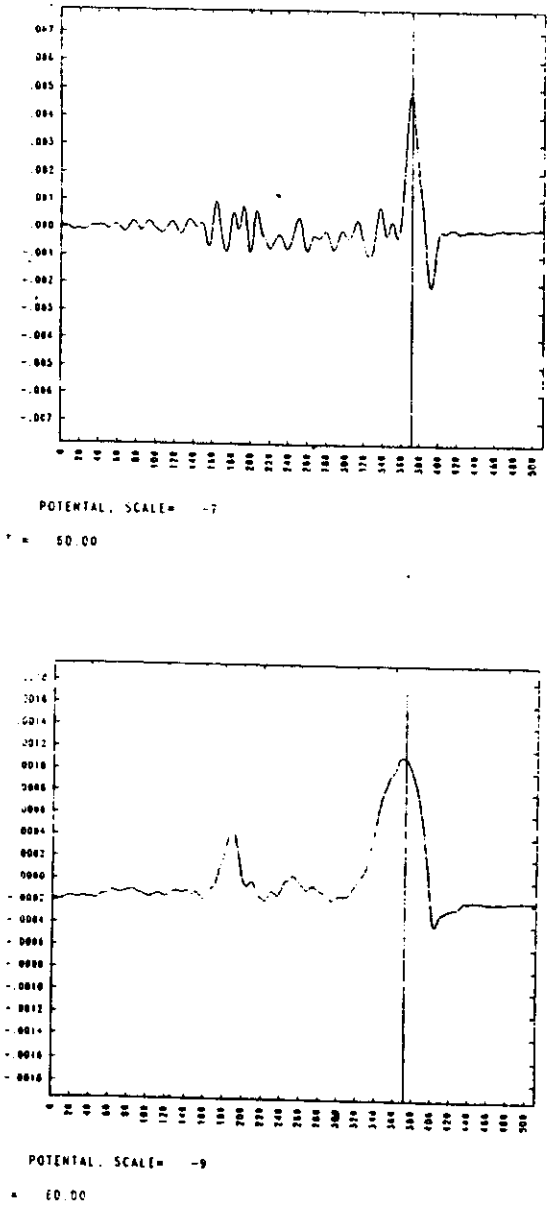

Fig. 4b Plasma wake emitted by one dimensional rest charge moving at velocity $3v_{te}$ using direct implicit model. Time step used is $\omega_p\Delta t = 2.0$ for the top panel and $\omega_p\Delta t = 10$ for the bottom panel. Electron -positron pair produced at x=150 in all cases.

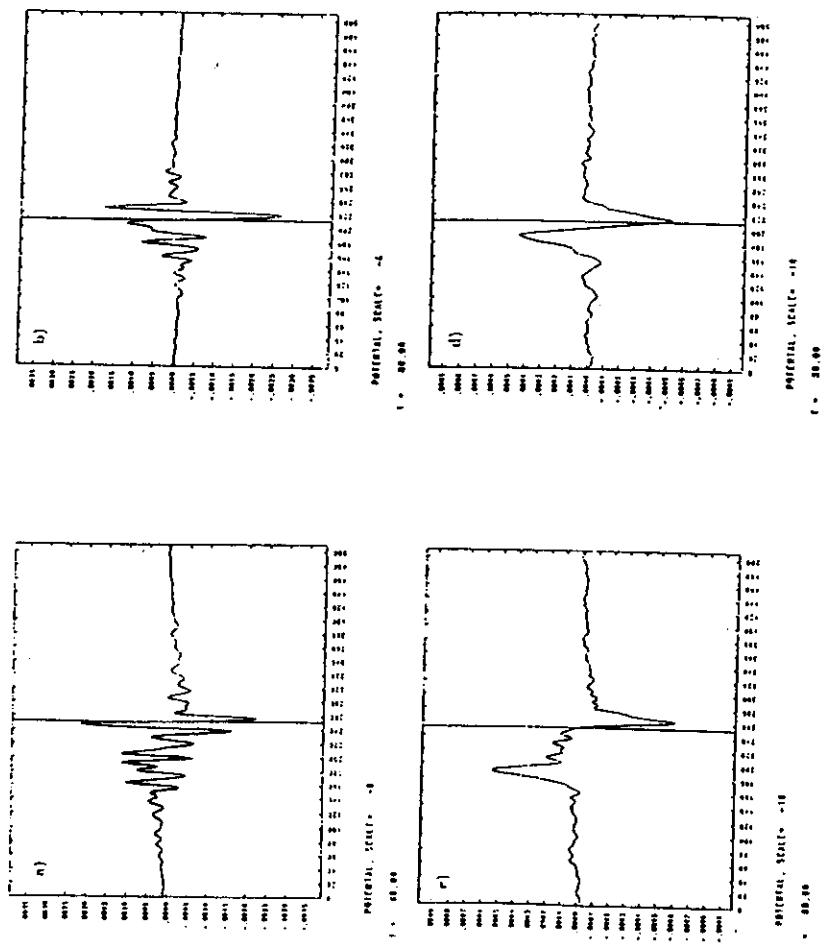

Fig. 5 Plasma wake emitted by one dimensional test charge moving at velocity v_{te} in panel a) and c) and at velocity $0.25v_{te}$ in b) and d) using direct implicit model. Time step used is $\omega_p\Delta t = 2$ for the top panels and $\omega_p\Delta t = 10$ for the bottom frames

5. Numerical Stochasticity

particles phase space location $(x, v) \xrightarrow[\text{(errors)}]{\text{mapping}} (x', v')$

- long time behavior of area-preserving integrators is considered

Leapfrog: $v^{n+1/2} = v^{n-1/2} - \Delta t \frac{\partial \phi(x^n)}{\partial x} \equiv F^n$

$$x^{n+1} = x^n + \Delta t\, v^{n+1/2}$$

Rewrite as:

$$v^{n+1} = v^n - \frac{\Delta t}{2}\left[\frac{\partial \phi}{\partial x}(x^n) + \frac{\partial \phi}{\partial x}(x^{n+1})\right]$$

$$x^{n+1} = x^n + \Delta t\, v^n - \frac{\Delta t^2}{2}\frac{\partial \phi}{\partial x}(x^n)$$

Using $\frac{\partial F(x^n)}{\partial x^n} = F'(x^{n+1})\left(1 + \frac{\Delta t^2}{2} F'(x^n)\right)$

$$\frac{\partial F(x^{n+1})}{\partial v^n} = \Delta t\, F'(x^{n+1})$$

Jacobian of trans $(x^n, v^n) \to (x^{n+1}, v^{n+1})$

$$J = \frac{\partial (x^{n+1}, v^{n+1})}{\partial (x^n, v^n)} = 1 \quad \therefore \text{Area pres.}$$

Harmonic well, freq. ω_0, dispersion relation: $\sin(\omega \Delta t/2) = \pm \omega_0 \frac{\Delta t}{2}$

$$(\Delta t_c) = \frac{2}{\omega_0} \quad \text{or} \quad \omega_0 \Delta t < 2$$

> 2 (odd even inst.)

$$\omega = \omega_0 \left[1 + \frac{(\omega_0 \Delta t)^2}{24} + \cdots\right]$$

Cumulative phase after N steps is $N\omega\Delta t$

so phase error: $N(\omega_0 \Delta)^3/24$

eg) ≤ 1 radian error $\Rightarrow \omega_0 \Delta t = 0.1$

$\therefore$ 24000 steps

$\omega_0 \Delta t = 0.3$

$\therefore$ 890 steps

$\phi(x) = A\cos(x)$

$$X^{n+1} = X^n + V^{n+1}$$
$$V^{n+1} = V^n + A\,\Delta t^2 \sin X^n$$

where $V^{n+1} = \Delta t\, V^{n+1/2}$
$V^n = \Delta t\, V^{n-1/2}$

Chirikov standard map: $\Theta^{n+1} = \Theta^n + I^{n+1}$
$I^{n+1} = I^n + K\sin\Theta^n$

$X \leftrightarrow \Theta$, $V \leftrightarrow I$, $A\Delta t^2 \leftrightarrow K$

Time-centered implicit

$$V^{n+1} = V^n - \frac{\Delta t}{2}\left[F(x^{n+1}) + F(x^n)\right]$$
$$X^{n+1} = X^n + \frac{\Delta t}{2}\left(V^{n+1} + V^n\right)$$

not an area preserving map (locally)

$(x^n, v^n) \to (x^{n+1}, v^{n+1})$

$$J = \left(1 - \frac{\Delta t^2}{4}F'(x^n)\right) \Big/ \left(1 - \frac{\Delta t^2}{4}F'(x^{n+1})\right)$$
$$\approx 1 - \frac{\Delta t^3 V^n}{4}F''(x^n)$$

$J \neq 1$ has no global consequences since change of phase space area in one place is made up for when particle moves in other direction.

Energy conserving mover

$$\dot{q} = \partial H/\partial p \;,\; \dot{p} = -\partial H/\partial q$$

$$\frac{q'-q}{\Delta t} = \frac{1}{2}\left[\frac{H(q',p')-H(q',p)}{p'-p} + \frac{H(q,p')-H(q,p)}{p'-p}\right]$$

$$\frac{p'-p}{\Delta t} = -\frac{1}{2}\left[\frac{H(q',p')-H(q,p')}{q'-q} + \frac{H(q',p)-H(q,p)}{q'-q}\right]$$

mult. 1st by $(p'-p)$ and second by $(q'-q)$

$$0 = H(q',p') - H(q,p)$$

$H = v^2/2 + \phi(x)$

$$\therefore \quad \frac{x^{n+1}-x^n}{\Delta t} = \frac{v^{n+1}+v^n}{2}$$

Pnts. of orbit fall on exact phase plane curves.

$$\frac{v^{n+1}-v^n}{\Delta t} = \begin{cases} -\dfrac{\phi(x^{n+1})-\phi(x^n)}{x^{n+1}-x^n}, & x^{n+1} \neq x^n \\ -\dfrac{\partial\phi}{\partial x}(x^n), & x^{n+1} = x^n \end{cases}$$

$$\frac{(v^{n+1})^2}{2} - \frac{(v^n)^2}{2} = \phi(x^n) - \phi(x^{n+1})$$

(1-D).